RSC Advances

ROYAL SOCIETY OF CHEMISTRY

www.rsc.org/advances

Journal Name

ARTICLE

Dendritic AIE-active luminogens with a POSS core: synthesis, characterization, and application as chemosensors

Received 00th January 20xx,
Accepted 00th January 20xx

DOI: 10.1039/x0xx00000x

www.rsc.org/

Kai Xiang,[ab] Lijuan He,[ab] Yanmin Li,[c] Caihong Xu,*[a] and Shuhong Li *[c]

Two nano-hybrid dendrimers were synthesized by grafted tetraphenylethene (TPE) units onto polyhedral oligomeric silsesquioxane (POSS) core through one-step hydrosilylation reaction. The two dendrimers demonstrated typical aggregation-induced emission (AIE) phenomenon, and they exhibited outstanding thermal stability and high fluorescence quantum yields. The emissions of their nanoaggregates can be quenched by picric acid or selectively by Ru^{3+} ion with a superamplification effect. The quenching constants of the dendrimers for picric acid and Ru^{3+} ion are as high as 560000 and 473640 M^{-1}, respectively, suggesting them highly sensitive chemosensors for explosives and metal ions.

Introduction

Since the pioneering work of Tang and co-workers,[1] the molecules with the property of aggregation-induced emission (AIE) have received increased attention both in academic research and industrial development.[2-7] The phenomenon of the AIE effect is opposite to the general belief of aggregation-caused quenching (ACQ)[8] of luminescence processes, and opens a new avenue for the development of novel luminescent materials with highly emissive in aggregation states. These materials have displayed high potential in the areas of optoelectronics,[9-12] chemical sensors,[13-15] and bioprobes.[16-19] Attracted by the fascinating phenomenon and its promising applications, many research groups have enthusiastically engaged in AIE studies. Synthesis of AIE-active luminogens (AIEgens) with various topological structures and exploring their new applications are the very important themes in the field of AIE research. Though AIEgens with various topological structures such as linear, zigzag, star-shaped, hyperbranched, and crosslinked structures were accessed,[20] dendritic AIEgens have rarely been reported in part due to dearth of appropriate scaffolds and difficulty of precise synthesis of well-defined and perfect 3D structures.[21-24]

On the other hand, due to its unique nanometer-sized structure, high thermal stability, and facile chemical modification, the cage-like polyhedral oligomeric silsesquioxane (POSS),[25] especially the highly symmetrical and topologically ideal cube octasilsesquioxae (T_8-POSS) with a cage size of approximately 0.5-0.7 nm,[26] has drawn intensive attention as a constructive unit for fabrication of various functional organic-inorganic hybrid materials. Design of new hybrid optoelectronic materials containing chromophore units covalently bounded to POSS has been an active research topic.[27] A large variety of POSS-containing fluorescent materials have been developed by combination of POSS and various chromophores in different modes, for example, attached mono-functionalized POSS as pendant groups onto conjugated polymers,[28] incorporated multi-functionalized POSS as a core in conjugated dendrimers and hyperbranched polymers.[29-31] These materials generally displayed improved quantum efficiencies, thermal properties, and color stabilities compared with their parent molecules without POSS unit. Recently, Tang and coworkers have introduced mono-functionalized POSS and tetraphenylethene (TPE) as pendant units onto polymer main chains and prepared AIE-active films. They further used to the films to detect explosive vapors.[32] However, to the best of our knowledge, there is no report on the dendritic AIEgens based on POSS precursors, in part because of the synthetic difficulty caused by large steric hindrance of POSS core and introduction of multi-functional groups simultaneously, as well as isolation of the well defined dendrimer.

In this work, we synthesized two organic-inorganic hybrid dendrimers, **POSS2** and **POSS4**, by decorating TPE units onto eight corners of T_8-POSS core through simple hydrosilylation reaction. The nano-hybrid materials have dramatically increased thermal stability compared with their parent TPE derivatives, and exhibited an obvious AIE characteristic. The new molecules showed improved luminescent quantum efficiencies in both dilute solution and solid states. Inspired by their AIE characteristic and 3D topological structure with a rigid scaffold, the two AIEgens were further used as chemosensors, which showed good sensitivity to picric acid (PA) and high selectivity to Ru^{3+} ion.

Results and discussion

Design and Synthesis. TPEs are nonplanar propeller-shaped luminogens. In a dilute solution, four phenyl rotors in a TP

[a] *Beijing National Laboratory for Molecular Sciences (BNLMS), Institute of Chemistry, Chinese Academy of Sciences, Beijing 100190, P. R. China.* E-mail: caihong@iccas.ac.cn
[b] *University of Chinese Academy of Sciences, Beijing, 100049, P. R. China*
[c] *School of Science, Beijing Technology and Business University, Beijing 100037, P. R. China,* lish@th.btbu.edu.cn
Electronic Supplementary Information (ESI) available: Supporting Information Available: preparation of compound **1** and **2**.
^{1}H, ^{13}C, ^{29}Si NMR spectra of synthetic compounds. See DOI: 10.1039/x0xx00000x

molecule undergo dynamic intramolecular rotations against its stator, which induces larger steric hindrance than planar molecule in synthesis of perfect dendrimer with a TPEgen on each corner of an inorganic T_8-POSS core. We designed the route of hydrosilylation reaction to achieve dendrtic AIEgen with POSS core. The synthetic routes to **POSS2** and **POSS4** are described in Scheme 1. **POSS2** was successfully synthesized via hydrosilylation reaction of **1** and **POSS1** in presence of Karstedt's catalyst in 83% isolated yield.[33] Similarly, **POSS4** was obtained from the reaction of **2** and **POSS3** in 32% isolated yield. The ^{1}H NMR spectra of **POSS4** indicates the ratio of E/Z-vinylene isomers is 1.7/1. The two isomers could not be isolated. **POSS2** and **POSS4** were easily purified by column chromatography. They were characterized by multinuclear (^{1}H, ^{13}C, ^{29}Si) NMR spectroscopy, FT-IR, and MALDI-TOF mass spectrometry. Both **POSS2** and **POSS4** possess good solubility in common organic solvents, such as hexane, dichloromethane, tetrahydrofuran, and toluene, but are insoluble in water and methanol.

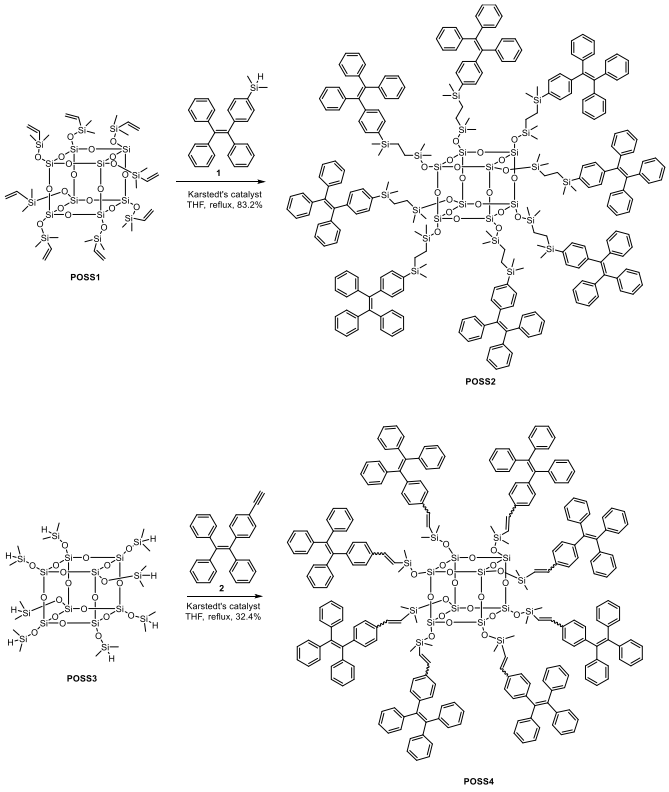

Scheme 1. Synthetic routes to **POSS2**, **POSS4**.

Thermal Properties and Morphology. Thermal stability of the organic optoelectronic materials is one of the most important factors which affects the device lifetime and reliability. The new organic-inorganic hybrid dendrimers exhibit outstanding thermal stability because of existence of POSS core. The thermogravimetric analysis (TGA) curves of **POSS2** and **POSS4** show the temperatures of 5% weight loss (T_d) around 450 °C in N_2 and above 355 °C in air (Figure 1) . The T_d is increased by about 200 °C in N_2 and 100 °C in air for dendrimers than those of their molecular counterparts. Solids **1** and **2** are crystalline, but after grafting onto POSS cage, the corresponding **POSS2** and **POSS4** show amorphous states. X-ray diffraction (XRD) spectra of **POSS2** and **POSS4** show a broad peak at about 2θ ≈ 19° (Figure 2). The differential scanning calorimetry (DSC) study also confirms the amorpous characteristics. Figure S1 shows the DSC curves for **1**, **2**, **POSS2** and **POSS4**. The DSC curves of **1** and **2** only show a sharp melting endothermal peak at 115 °C and 157 °C, respectively (Figure S1, A). A glass transition (T_g) peak at 62 °C appears for **POSS2** (Figure S1, B). No evidence of a glass transition for **POSS4** was observed up to 400 °C (Figure S1, B).

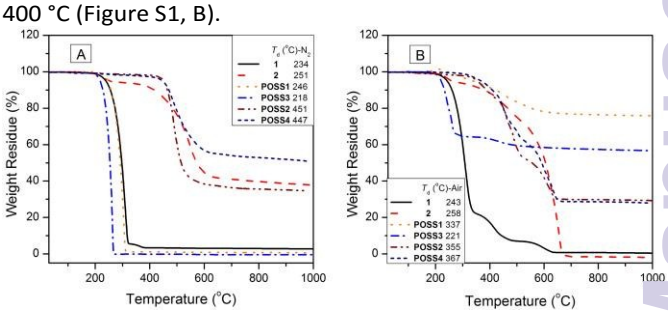

Figure 1. TGA curves of **1**, **2**, **POSS1**, **POSS2**, **POSS3**, **POSS4** under N_2 (A) or air (B) at a heating rate of 10 °C/min.

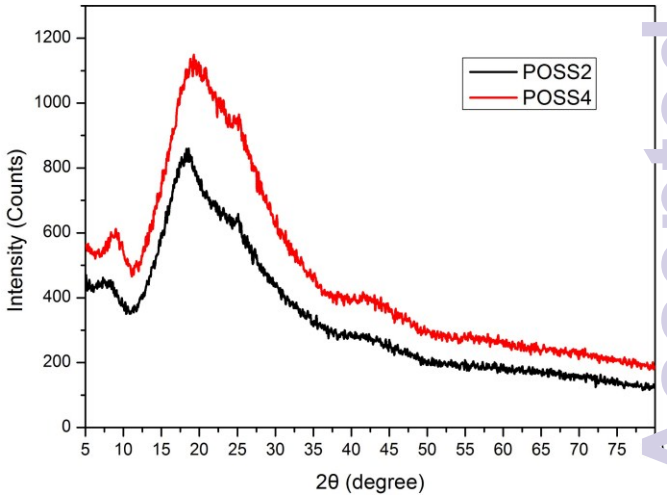

Figure 2. XRD patterns of **POSS2** and **POSS4**.

Photophysical Properties. Figure 3 shows the UV-vis spectra of **POSS2** and **POSS4** in their dilute THF solutions, together with the data of **1** and **2**, for comparison. The dendrimers exhibit absorption peaks inherent to their parent molecular counterparts. **POSS2** shows the same absorption maximum at 313 nm as that of **1**. The absorption maximum of **POSS4** is located at 324 nm, which slightly red-shifts 4 nm from 320 nm of **2**.

To check whether the dendrimers were AIEgens, their fluorescent behaviors in THF and THF-water mixture with different water fraction were studied (Figure 4). The photoluminescence (PL) spectrum of **POSS2** in THF is basically a flat line parallels to the abscissa, indicating its nonemissive character in the solution state (Figure 4A and 4C). However, when large amounts of water, the poor solvent, were added into its THF solution, intense PL spectra with an emission peak at 486 nm were observed. This fact suggests formation of the aggregates in mixed solvents. From the molecular solution in THF to the aggregate state in 90% aqueous solution, the emission intensity of **POSS2** was increased by 322-fold. Similar

emission behavior was also observed for **POSS4**. The emission spectra of **POSS4** in THF-water mixtures are displayed in Figure 4B. Its emission peak emerges at 492 nm as the water fraction up to 50%. At 90% water content, the emission intensity of **POSS4** was increased by 458-fold with 6 nm blue-shift in the emission maximum. These results confirm that POSS-cored luminogens **POSS2** and **POSS4** are AIE-active.

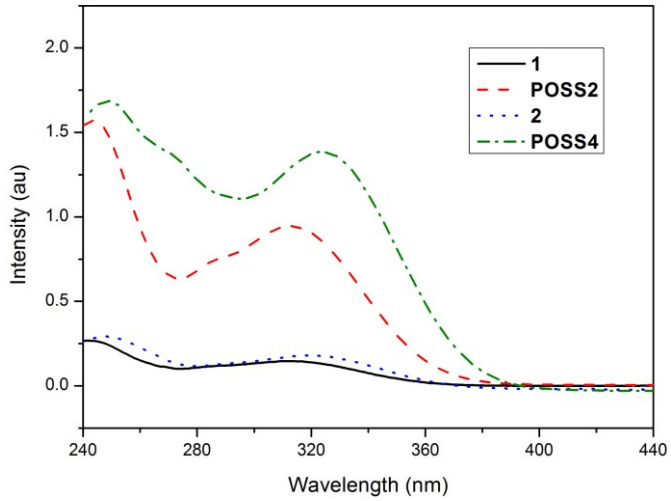

Figure 3. Absorption spectra of THF solutions of **1**, **2**, **POSS2**, **POSS4**. Solution concentration: 10 μM.

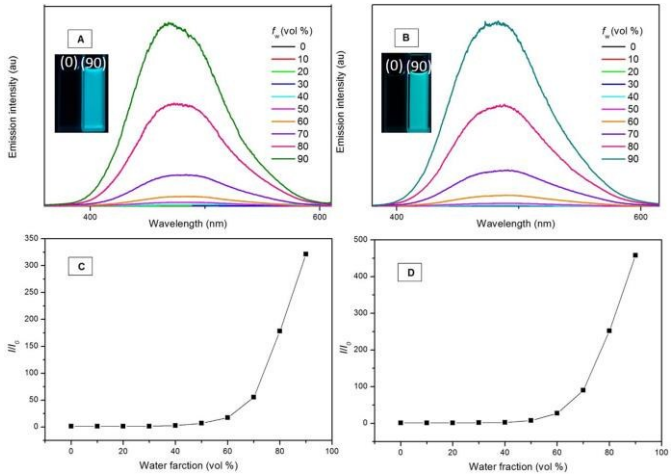

Figure 4. Emission spectra of **POSS2** (A), **POSS4** (B) in THF-water mixtures. (C), (D) Plot of (I/I_0) values versus the compositions of the aqueous mixtures. I_0 = emission intensity in pure THF solution. Solution concentration: 10 μM; excitation wavelength: 315 nm for **POSS2**, and 320 nm for **POSS4**. Inset: photographs of **POSS2** and **POSS4** in THF and THF/water (1:9 *v*/*v*) mixture taken under illumination of a handheld UV lamp.

To confirm the formation of nanoparticles in THF/H_2O mixtures with high water contents, particle size analysis was carried out (Figure 5). The average sizes for the nanoparticles of **POSS2** formed in 60, 70, 80, and 90% aqueous mixtures are 285.1, 266.6, 247.7, and 151.8 nm, respectively (Figure 5A). With increase of the amount of water, the sizes of the particles decreased. This result may be explained as follow: When small amount of water was added to THF solution of **POSS2**, only limited **POSS2** formed aggregation, which served as cluster centers of other dissolved molecules and slowly formed large nanoaggregates. When large amount of water was added, more **POSS2** aggregated quickly, forming nanoparticles of smaller sizes. A similar result was also found for **POSS4** (Figure 5B).

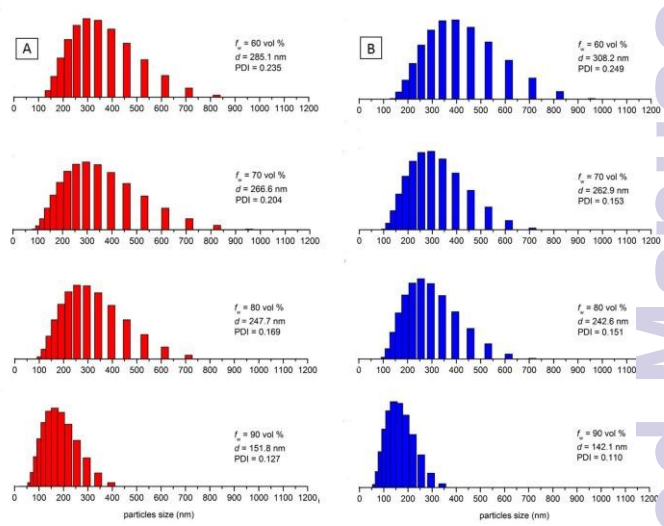

Figure 5. Particle size distributions of aggregates of **POSS2** (A) and **POSS4** (B) suspended in THF/water mixtures with water fractions (f_w) of 60, 70, 80 and 90 vol %. Abbreviation: *d* = *Z*-average diameter, PDI = polydispersity.

The nano-size POSS core can improve the fluorescence quantum yield (Φ_F) of AIEgens both in solution and solid state. The Φ_F values of the thin solid films of **POSS2** and **POSS4** are 44.3% and 55.6%, respectively, which are higher than the data of **1** and **2** around 6.6% and 9.5%, respectively. The Φ_F values of **POSS2** and **POSS4** in the solution state are still low (0.46% and 0.48%, respectively, table 1), though the growth rates of which are 64% and 41%, respectively, based on the data of their parent TPE derivatives (0.28% and 0.34%, respectively, table 1). The possible reason is: in solution, though the nano-sized POSS core contributes to aggregation, the relatively long linkage between TPE unit and POSS core can provide enough space for the intramolecular rotation (IMR) of the aromatic rotors in the AIEgens. IMR consumes the excited state energy of the AIEgens and results the weakly fluorescence in the solution. In solid state, the IMR is restricted, which is the main cause for AIE effect. Furthermore, the rigid and bulky POSS core aligns TPEs in a radial fashion relative to the core and isolates them from each other, which reduces intermolecular interactions and increase emission efficiency. The two reasons result in higher quantum yields of **POSS2** and **POSS4** in the solid state.

Table 1. Optical and thermal properties of **1**, **2**, **POSS2** and **POSS4**.

	λ_{abs}/ nm[a]	λ_{em}/ nm[a]	Φ_F (%)		T_d (℃)[d]	
			(Soln)[b]	(Film)[c]	N_2	Air
1	313	485	0.28	37.7	234	243

POSS2	313	486	0.46	44.3	451	355
2	320	487	0.34	46.1	251	258
POSS4	324	493	0.48	55.6	447	367

[a] In THF solution (Soln，10 μM). [b] Determined using quinine sulfate (Φ_F = 55% in 0.1M sulfuric acid) as standard .[c] Film drop-cast on a quartz plate. Determined by an integrating sphere. [d] Determined by TGA at 5% mass loss, 10 °C/min in N_2 or air.

Explosive Detection. The detection of explosives such as 2,4,6-trinitrotoluene (TNT), 2,4-dinitrotoluene (DNT), 1,3,5-trinitro-perhydro-1,3,5-triazine (RDX), and PA, has become an increasingly important and urgent issue for environmental protection and homeland security. Among detection techniques, fluorescence sensing of explosives has attracted the most attention because it's more simple, sensitive, and selective. TPE derivatives has displayed their potentials in detection of explosives,[34,35] so we expected the new POSS-cored dendrimers have higher sensitivity due to existence of eight TPE units in one molecule. The application of the new AIEgens as chemosensors for detection of explosives was then examined. The nanoaggregates of the compounds in THF-water mixtures with 90% water contents were utilized as probes. Commercial available PA was employed as a model compound. As shown in Figure 6A and Figure 6B, the emission intensities were progressively decreased, when PA was gradually added into the nanoaggregates of **POSS2** or **POSS4** in aqueous mixtures with the solution concentration as low as 1 μM. The PL quenching of **POSS2** and **POSS4** were discerned at a PA concentration as low as 5.7 μM or 1.3 ppm. When the PA concentration was increased to 0.86 mM, no emission was observed from the aqueous mixtures. The Stern-Volmer plots of I_0/I-1 of **POSS2** and **POSS4** versus PA concentration were shown in Figure 6C and Figure 6D to further quantify the quenching efficiency. The plots showed upward-bending curves and were composed of three stages, indicating that the PL quenching became more efficient with increasing quencher concentration.[36,37] The largest quenching constants of **POSS2** and **POSS4** were up to 560000 M^{-1} and 376000 M^{-1}, respectively. Notably, their quenching constants for PA are much higher than that of TPE-based monomers (34000 M^{-1}),[38] as well as that of linear polysiloles and polygermoles reported in the literature (6710-11000 M^{-1}).[39] The dendritic **POSS2** and **POSS4** possess 3D topological structures with rigid POSS scaffold, which contain more molecular cavities to capture PA molecules by electron and/or energy transfer complexation.[40,41] As expected, the dendritic **POSS2** and **POSS4** can be used as highly sensitive fluorescent chemsensors for explosive detection.

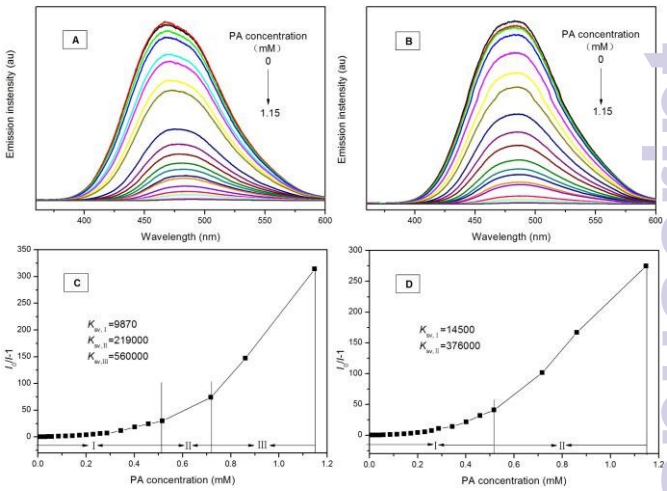

Figure 6. Emission spectra of **POSS2** (A), **POSS4** (B) in THF-water mixtures with 90% water contents containing different amounts of PA. Solution concentration: 1 μM; excitation wavelength: 315 nm to **POSS2**, 320 nm to **POSS4**. (C) Stern-Volmer plot of I_0/I-1 of **POSS2** (C) and **POSS4**. (D) versus PA concentration in THF-water mixtures with 90% water contents and K_{sv} values in different concentration regions. I_0 = PL intensity at [PA] = 0 mM.

Metal-Ion Sensors. Ruthenium(Ⅲ) complexes are catalysts in olefin metathesis reactions, but they are corrosive and destructive to the respiratory tract, eyes, skin, and digestive tract. Development of highly sensitive and selective sensors to detect Ru^{3+} ion is in great demand in view of the environmental protection. The reported method to detect Ru^{3+} ion is mainly focused on inductively coupled plasma mass spectrometry (ICP-MS), which requires sophisticated operation and time-consuming sample preparation, but has limited sensitivity.[42] Fluorescent chemosensors could be an alternative method for Ru^{3+} ion detection, but the known fluorescent probes for Ru^{3+} ion are quite rare. To the best of our knowledge, there are only four reports concerning fluorescent probes for Ru^{3+} ion, one is based on fluorescein derivative,[43] the others are AIEgens.[11,44,45] **POSS2** and **POSS4** show typical AIE characteristics and high fluorescence quantum yields, we guessed the dendritic AIEgens may be good sensitive and selective fluorescence chemosensors for Ru^{3+} ion detection with lower detection limit. To know it, the relative investigation was performed.

The nanoaggregates of the compounds in THF-water mixtures with 90% water contents were utilized as probes. With the gradual addition of Ru^{3+} ion to the nanoparticle suspensions, the emissions of **POSS2** and **POSS4** decreased progressively (Figure 7). The PL quenching can be clearly recognized at a low Ru^{3+} ion concentration of 0.2 μM or 20.2 ppb. Compared with the reported reults of AIEgens-based fluorescent probes for Ru^{3+} ion (around 1 ppm), this is an exciting result, which is the lowest detection concentration in the known AIE chemosensors.[11,44,45] At [Ru^{3+}] = 20 μM, the PL intensity of **POSS2** is merely 37% of its original value. At the same ion concentration, the emissions of **POSS4** are almost quenched

completely, showing a 5-fold higher sensitivity than **POSS2**. Electrostatic interaction or charge-transfer complexation between electron-rich **POSS2** (**POSS4**) and electron-deficient Ru^{3+} may account for PL annihilation. The Stern-Volmer plot of I_0/I-1 of **POSS2** and **POSS4** versus Ru^{3+} ion concentration gave an upward bending curve instead of a linear line, indicating a superamplified quenching effect. The Stern-Volmer curves of **POSS2** and **POSS4** can be well fitted to the exponential equations of I_0/I=1.75e$^{41898[Ru3+]}$ -0.91 and I_0/I=11.3e$^{41915[Ru3+]}$ - 11.6, with quenching constants of about 73322 $M^{-1}$and 473640 M^{-1}, respectively.

To evaluate the selectivity of **POSS2** and **POSS4** toward Ru^{3+} detection, we studied the PL change of the dendrimers in presence of other metal ions. As shown in Figure 8, addition of other metal ions, including Mg^{2+}, Fe^{2+}, Fe^{3+}, Co^{2+}, Ni^{2+}, Cu^{2+}, Zn^{2+}, Rh^{3+}, Cd^{2+}, Pd^{2+}, Hg^{2+}, exerts little change on the PL of **POSS2** and **POSS4**, which indicates the high selectivity of the dendrimers to Ru^{3+}. Although the reason for such selectivity remains unclear at present, we think that the higher standard reduction potential of the Ru (Ⅲ) / Ru (0) couple relative to other cation / metal systems may be responsible for such selective sensing.[11,44,45]

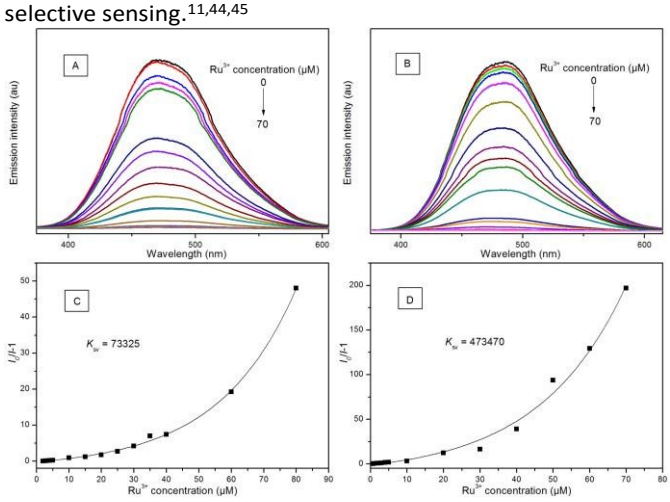

Figure 7. (A) Emission spectra of **POSS2** (A), **POSS4** (B) in THF-water mixtures with 90% water contents containing different amounts of Ru^{3+} ion. Solution concentration: 10 μM; excitation wavelength: 315 nm to **POSS2**, 320 nm to **POSS4**. (C) Stern-Volmer plot of I_0/I-1 of **POSS2** (C) and **POSS4**. (D) versus Ru^{3+} ion concentration in THF-water mixtures with 90% water contents and K_{sv} values. I_0 = PL intensity at [Ru^{3+}] = 0 μM.

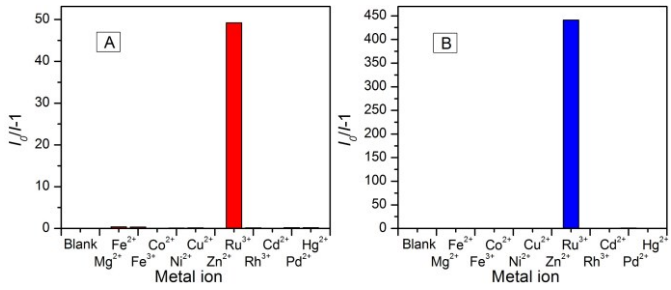

Figure 8. Changes in relative emission intensities (I_0/I − 1) of **POSS2** (A) and **POSS4** (B) in THF/H_2O mixtures (1:9 by volume; concentration =10 μM) with various metal ions (100 μM). I_0 = intensity in the absence of metal ions.

Conclusions

In summary, we have successfully synthesized two novel nano-hybrid dendrimers **POSS2** and **POSS4**, with eight TPE units bonded to a POSS core by convenient one-step hydrosilylation reaction. The nano-hybrid materials exhibit AIE properties with many attractive merits for application as organic optoelectronic materials. 3D topological structures of **POSS2** and **POSS4** allowed them possess more molecular cavities or voids than organic small molecules or linear polymers for analyte capturing and diffusion pathways for exciton migration making them attractive chemosensors. The emissions of nanoaggregates of the new AIEgens could be quenched efficiently by PA and Ru^{3+} ion with a superamplification effect, suggesting them promising for application in the detection of explosives and metal ions.

Experimental

Unless otherwise mentioned, materials were obtained from commercial suppliers and used without further purification. The key starting compounds **1**,[46] **2**,[46] **POSS1**,[47] and **POSS3**[48] were synthesized according to previous published procedures, respectively. Karstedt's catalyst was received from Aldrich. Tetrahydrofuran (THF) was dried by distillation over sodium metal prior to use.

The UV-vis and fluorescence spectra were recorded with TU-1900 spectrophotometer and Hitachi F-4500 spectrofluorophotometer, respectively. The FT-IR spectra were recorded with Bruker Tensor 27 FT-IR spectrometer. ^{1}H and ^{13}C NMR was recorded on Bruker Avance III 400 HD spectrophotometer using $CDCl_3$ as solvent. ^{29}Si NMR was recorded on Bruker DMX 300 spectrophotometer. Chemical shifts are referenced to the solvent peak (for $CDCl_3$, ^{1}H NMR: 7.26 ppm, ^{13}C NMR: 77.0 ppm) and TMS (^{29}Si); Data are reported as follows: chemical shifts in ppm (δ), multiplicity (s = singlet, d = doublet, quint = quintet, m = multiplet), integration. Absolute fluorescent (PL) quantum yield was tested on Hamamatsu C11347 spectrometer. TGA was carried on Hitachi STA 7300 under N_2 or air at a heating rate of 10 °C/min. DSC was carried on Seiko EXSTAR DSC6220 under N_2 at a heating rate of 10 °C/min. High-resolution mass spectra (HRMS) were recorded with Bruker SolariX 9.4T spectrometer operating in MALDI-FT mode. The particle sizes of the aggregates were measured on Zetasizer Nano ZS ZEN 3600. XRD was recorded on PANalytical Empyrean.

Preparation of compound POSS2. To a THF (1 ml) solution of **POSS1** (30.7 mg, 0.025 mmol, 1.0 eq.) and **1** (127 mg, 0.325 mmol, 13 eq.) was added Karstedt's catalyst. The reaction mixture was stirred at room temperature for 30 min and warmed to 80 °C. After refluxed for 24 h, the reaction mixture was concentrated vacuum to get residue. The residue was purified by silica gel column chromatography using petroleum ether/dichloromthane = 8:1 as eluent to give 90.5 mg (83.2 %) of compound **POSS2** as a white solid. ^{1}H NMR (400 MHz, $CDCl_3$), δ (ppm): 7.21 (d, 16H, Ar-H), 7.09-6.98 (m, 136H, Ar-H), 0.63-0.58 (m, 16H, CH_2), 0.47-0.43 (m, 16H, CH_2), 0.19 (s, 48H, CH_3),

0.09 (s, 48H, CH_3). ^{13}C NMR (100 MHz, $CDCl_3$), δ (ppm): 143.0, 143.8, 143.7, 141.0, 137.2, 132.9, 131.3, 130.5, 127.6, 126.4, 126.3, 9.6, 6.8, -0.9, -3.5. ^{29}Si NMR ($CDCl_3$, 60MHz), δ (ppm):δ 6.6, -8.4, -115.6. IR (KBr), υ (cm^{-1}): 3054, 3019, 2956, 2908, 1612, 1410, 1252 (Si-CH_3 bending), 1090 (Si-O-Si stretching), 830 (Si-CH_3 stretching), 699, 554. HRMS (MALDI-TOF): m/z ($[M+Na]^+$) = 4368.55254 (calcd for $C_{256}H_{280}O_{20}Si_{24}Na$=4368.52467).

Preparation of compound POSS4. The product was synthesized according to the procedure as described above for synthesis of **POSS2**, giving a yellow solid of the product **POSS4** in 32.4% yield. ^1H NMR (400 MHz, $CDCl_3$), δ (ppm): 7.16-7.07 (m, 36H, Ar-H), 7.07-6.96 (m, 95H, Ar-H), 6.96-6.89 (m, 21H, Ar-H), 6.83 (d, 6H, E-ArCH= and Ar-H), 6.25 (dd, 5H, E-SiCH=), 5.78 (s, 3H, Z-ArCH=), 5.68 (s, 3H, Z-SiCH=), 0.17 (d, 48H). ^{13}C NMR (100 MHz, $CDCl_3$), δ (ppm): 150.1, 144.6, 143.8, 143.7, 143.6, 143.6, 141.9, 141.1, 140.8, 140.8, 140.6, 135.9, 131.5, 131.4, 131.3, 131.2, 127.7, 127.6, 126.5, 126.4, 126.4, 126.1, 0.37, 0.25. ^{29}Si NMR ($CDCl_3$, 60MHz), δ (ppm): -5.4, -6.2, -116.0. IR (KBr), υ (cm^{-1}): 3061, 2960, 1609, 1256 (Si-CH_3 bending), 1167, 1089 (Si-O-Si stretching), 849 (Si-CH_3 stretching), 764, 700, 561. HRMS (MALDI-TOF): m/z ($[M+Na]^+$)=3888.20435 (calcd for $C_{240}H_{216}O_{20}Si_{16}Na$=3888.20854).

Preparation of Metal-Ion Solutions. Inorganic salts (magnesium chloride, iron (II) chloride, iron (III) chloride, cobalt (II) chloride, nickel(II) chloride hexahydrate, copper(II) chloride, zinc chloride, ruthenium(III) chloride, rhodium(III) chloride, cadmium chloride, Mercury(II) nitrate hydrate were dissolved in distilled water (5 mL) to afford 50 mM aqueous solutions. The stock solutions were diluted to the desired concentrations with distilled water for further experiments.

Acknowledgements

The authors gratefully acknowledge the National Natural Science Foundation of China (NSFC, Nos. 50673094 and 20774102) for financial support.

Notes and references

1 J. D. Luo, Z. L. Xie, J. W. Y. Lam, L. Cheng, H. Y. Chen, C. F. Qiu, H. S. Kwok, X. W. Zhan, Y. Q. Liu, D. B. Zhu and B. Z. Tang, *Chem. Commun.*, 2001, 1740-1741.
2 Y. N. Hong, J. W. Y. Lam and B. Z. Tang, *Chem. Commun.*, 2009, 4332-4353.
3 Y. N. Hong, J. W. Y. Lam and B. Z. Tang, *Chem. Soc. Rev.*, 2011, **40**, 5361-5388.
4 D. Ding, K. Li, B. Liu and B. Z. Tang, *Acc. Chem. Res.*, 2013, **46**, 2441-2453.
5 J. Mei, Y. N. Hong, J. W. Y. Lam, A. J. Qin, Y. H. Tang and B. Z. Tang, *Adv. Mater.*, 2014, **26**, 5429-5479.
6 R. T. K. Kwok, C. W. T. Leung, J. W. Y. Lam and B. Z. Tang, *Chem. Soc. Rev.*, 2015, **44**, 4228-4238.
7 J. Liang, B. Z. Tang and B. Liu, *Chem. Soc. Rev.*, 2015, **44**, 2798-2811.
8 J. B. Birks, *Photophysics of Aromatic Molecules*, Wiley, London, 1970
9 S. J. Liu, F. Li, Q. Diao and Y. G. Ma, *Org. Electron.*, 2010, **11**, 613-617.
10 J. Mei, J. Wang, J. Z. Sun, H. Zhao, W. Z. Yuan, C. M. Deng, S. M. Chen, H. H. Y. Sung, P. Lu, A. J. Qin, H. S. Kwok, Y. G. Ma, I. D. Williams and B. Z. Tang, *Chem. Sci.*, 2012, **3**, 549-558.
11 C. Y. K. Chan, Z. J. Zhao, J. W. Y. Lam, J. Z. Liu, S. M. Chen, P. Lu, F. Mahtab, X. J. Chen, H. H. Y. Sung, H. S. Kwok, Y. G. Ma, I. D. Williams, K. S. Wong and B. Z. Tang, *Adv. Funct. Mater.*, 2012, **22**, 378-389.
12 Z. F. Chang, Y. B. Jiang, B. R. He, J. Chen, Z. Y. Yang, P. Lu, H. S. Kwok, Z. J. Zhao, H. Y. Qiu and B. Z. Tang, *Chem. Commun.*, 2013, **49**, 594-596.
13 M. Wang, G. X. Zhang, D. Q. Zhang, D. B. Zhu and B. Z. Tang, *J. Mater. Chem.*, 2010, **20**, 1858-1867.
14 T. Y. Han, J. W. Y. Lam, N. Zhao, M. Gao, Z. Y. Yang, E. G. Zhao, Y. P. Dong and B. Z. Tang, *Chem. Commun.*, 2013, **49**, 4848-4850.
15 X. J. Chen, X. Y. Shen, E. J. Guan, Y. Liu, A. J. Qin, J. Z. Sun and B. Z. Tang, *Chem. Commun.*, 2013, **49**, 1503-1505.
16 S. Kim, H. E. Pudavar, A. Bonoiu and P. N. Prasad, *Adv. Mater.*, 2007, **19**, 3791-3795.
17 Y. Hong, L. Meng, S. Chen, C. W. T. Leung, L.-T. Da, M. Faisal, D.-A. Silva, J. Liu, J. W. Y. Lam, X. Huang and B. Z. Tang, *J. Am. Chem. Soc.*, 2011, **134**, 1680-1689.
18 Y. Yu, C. Feng, Y. Hong, J. Liu, S. Chen, K. M. Ng, K. Q. Luo and B. Z. Tang, *Adv. Mater.*, 2011, **23**, 3298-3302.
19 W. Qin, D. Ding, J. Z. Liu, W. Z. Yuan, Y. Hu, B. Liu and B. Z. Tang, *Adv. Funct. Mater.*, 2012, **22**, 771-779.
20 R. R. Hu, N. L. C. Leung and B. Z. Tang, *Chem. Soc. Rev.*, 2014, **43**, 4494-4562.
21 K. Shiraishi, T. Kashiwabara, T. Sanji and M. Tanaka, *New J. Chem.*, 2009, **33**, 1680-1684.
22 S. S. Li, T. H. Leng, H. B. Zhong, C. Y. Wang and Y. J. Shen, *J. Heterocyclic Chem.*, 2012, **49**, 64-70.
23 M. K. Leung, Y. S. Lin, C. C. Lee, C. C. Chang, Y. X. Wang, C. P. Kuo, N. Singh, K. R. Lin, C. W. Hu, C. Y. Tseng and K. C. Ho, *RSC Adv.*, 2013, **3**, 22219-22228.
24 B. Xu, J. B. Zhang, H. H. Fang, S. Q. Ma, Q. D. Chen, H. B. Sun, C. Im and W. J. Tian, *Poly. Chem.*, 2014, **5**, 479-488.
25 R. H. Baney, M. Itoh, A. Sakakibara and T. Suzuki, *Chem. Rev.*, 1995, **95**, 1409-1430.
26 D. B. Cordes, P. D. Lickiss and F. Rataboul, *Chem. Rev.*, 2010, **110**, 2081-2173.
27 K. L. Chan, P. Sonar and A. Sellinger, *J. Mater. Chem.*, 2009, **19**, 9103-9120.
28 S. Xiao, M. Nguyen, X. Gong, Y. Cao, H. B. Wu, D. Moses and A. J. Heeger, *Adv. Funct. Mater.*, 2003, **13**, 25-29.
29 C. B. He, Y. Xiao, J. C. Huang, T. T. Lin, K. Y. Mya and X. H. Zhang, *J. Am. Chem. Soc.*, 2004, **126**, 7792-7793.
30 A. Sellinger, R. Tamaki, R. M. Laine, K. Ueno, H. Tanabe, E. Williams and G. E. Jabbour, *Chem. Commun.*, 2005, 3700-3702.
31 J. C. Furgal, J. H. Jung, T. Goodson and R. M. Laine, *J. Am. Chem. Soc.*, 2013, **135**, 12259-12269.
32 H. Zhou, Q. Ye, W. T. Neo, J. Song, H. Yan, Y. Zong, B. Z. Tang, T. S. A. Hor and J. W. Xu, *Chem. Commun.*, 2014, **50**, 13785-13788.
33 B. Marciniec, *Hydrosilylation: A Comprehensive Review on Recent Advances*. Springer Science, 2009.

34 A. J. Qin, J. W. Y. Lam, L. Tang, C. K. W. Jim, H. Zhao, J. Z. Sun and B. Z. Tang, *Macromolecules*, 2009, **42**, 1421-1424.
35 C. Y. K. Chan, J. W. Y. Lam, C. M. Deng, X. J. Chen, K. S. Wong and B. Z. Tang, *Macromolecules*, 2015, **48**, 1038-1047.
36 J. Z. Liu, Y. C. Zhong, J. W. Y. Lam, P. Lu, Y. N. Hong, Y. Yu, Y. N. Yue, M. Faisal, H. H. Y. Sung, I. D. Williams, K. S. Wong and B. Z. Tang, *Macromolecules*, 2010, **43**, 4921-4936.
37 R. R. Hu, J. W. Y. Lam, M. Li, H. Q. Deng, J. Li and B. Z. Tang, *J. Polym. Sci., Part A: Polym. Chem.*, 2013, **51**, 4752-4764.
38 D. D. Li, J. Z. Liu, R. T. K. Kwok, Z. Q. Liang, B. Z. Tang and J. H. Yu, *Chem. Commun.*, 2012, **48**, 7167-7169.
39 H. Sohn, M. J. Sailor, D. Magde and W. C. Trogler, *J. Am. Chem. Soc.*, 2003, **125**, 3821-3830.
40 S. Zahn and T. M. Swager, *Angew. Chem., Int. Ed.*, 2002, **41**, 4225-4230.
41 Z. J. Zhao, Y. J. Guo, T. Jiang, Z. F. Chang, J. W. Y. Lam, L. W. Xu, H. Y. Qiu and B. Z. Tang, *Macromol. Rapid Commun.*, 2012, **33**, 1074-1079.
42 D. Beauchemin, *Anal. Chem.*, 2008, **80**, 4455-4486.
43 B. Chen, F. Song, S. Sun, J. Fan and X. Peng, *Chem. – Eur. J.*, 2013, **19**, 10115-10118.
44 C. Y. K. Chan, J. W. Y. Lam, C. K. W. Jim, H. H. Y. Sung, I. D. Williams and B. Z. Tang, *Macromolecules*, 2013, **46**, 9494-9506.
45 H. Q. Deng, R. R. Hu, E. G. Zhao, C. Y. K. Chan, J. W. Y. Lam and B. Z. Tang, *Macromolecules*, 2014, **47**, 4920-4929.
46 J. Wang, J. Mei, E. G. Zhao, Z. G. Song, A. J. Qin, J. Z. Sun and B. Z. Tang, *Macromolecules*, 2012, **45**, 7692-7703.
47 S. E. Yuchs and K. A. Carrado, *Inorg. Chem.*, 1996, **35**, 261-262.
48 M. Dutkiewicz, H. Maciejewski, B. Marciniec and J. Karasiewicz, *Organometallics*, 2011, **30**, 2149-2153.